

Hierarchical Composite Grid Method for Global-Local Analysis of Laminated Composite Shells

J.Fish, A.Suvorov and V.Belsky

*Department of Civil Engineering and Scientific Computation Research Center
Rensselaer Polytechnic Institute
Troy, NY, 12180, USA*

ABSTRACT

A hierarchical version of the composite grid method (denoted as HFAC), which exploits the solution of the shell model in studying local effects via 3D solid model, is developed. Convergence studies on a beam/2D model problem indicate that the spectral radius of the point iteration matrix for the HFAC method is $O(1)$ and $O((L/H)^2)$ with exact and approximate auxiliary coarse grid solutions, respectively, where L and H are the span and the thickness of the beam, respectively. Numerical experiments in multi-dimensions confirm these findings.

1.0 Introduction

Global-local techniques for laminated composite shells, which merge the Equivalent Single Layer (ESL) model aimed at predicting overall response with Discrete Layer (DL) model intended for capturing local effects, are recently receiving an increasing attention. We refer to [22] for a comprehensive review of global-local techniques for composite laminates and to [7] and [8] for various aspects of reliability, convergence and accuracy of global-local techniques.

In this paper, we are focusing only on the class of global-local techniques that advocates a hierarchical solution strategy in the sense that information from the analysis of an ESL model is exploited in the resolution of local effects using a DL model. Among the most popular hierarchical global-local strategies are the various forms of multigrid and composite grid methods [14]-[19], [30] as well as the methods based on hierarchical decomposition of approximation space [1]-[6], [20]-[22]. Recently, the composite grid method originated for displacement-based linear systems, has been extended to hybrid systems [26]. Engineering global-local approaches, which approximate a detailed response by means of post processing techniques, such as subjecting refined discrete layer model to the boundary conditions extracted from the global ESL model, can be viewed as

a single iteration within the composite grid procedure. For various improvements of this simple “zoom” technique, we refer to [23]-[25].

The present paper presents a hierarchical version [18] of the composite grid method (denoted as HFAC) [14], which exploit the solution of the shell model in the process of solving a coupled global-local problem. The outline of the paper is as follows: In section 2 the principles of the composite grid method are outlined in the context of laminated plates and shells. A convergence analysis on a model beam/2D problem is carried out in Section 3. These studies show that the spectral radius of the point iteration matrix for the HFAC method is $O(1)$ and $O((L/H)^2)$ with exact and approximate auxiliary coarse grid solutions, respectively, where L and H are the span and the thickness of the beam, respectively. Numerical studies in multidimensions conclude the manuscript.

2.0 Hierarchical Composite Grid Method

In this section, we present the formulation of a global-local solution algorithm for problems where one or more regions, requiring a detailed local resolution, are modeled as a 3D solid model, whereas elsewhere the shell model is used.

2.1 Problem definition and notation

We adopt the notation introduced in [18][26]. Consider a finite element mesh \tilde{G} consisting of shell elements on $\tilde{\Omega}$, which is a dimensionally reduced domain of Ω as shown in Figure 1. Let G be a 3D solid finite element mesh placed on the subregion $\Omega_L \in \Omega$. The composite grid consists of the shell model in the complement of $\tilde{\Omega}_L$ in $\tilde{\Omega}$, and the 3D solid mesh on Ω_L .

We partition the 3D solid mesh G (subsequently referred to as the fine or local grid) as

$$G = G_I \cup G_L \tag{1}$$

where G_I represents the interface degrees of freedom in Ω_I , and G_L the internal degrees of freedom. The mesh consisting of shell elements (coarse or auxiliary grid) is partitioned as follows:

$$\tilde{G} = \tilde{G}_I \cup \tilde{G}_L \cup \tilde{G}_G \tag{2}$$

where \tilde{G}_I represents the degrees of freedom associated with the coarse finite element nodes at the interface $\tilde{\Omega}_I$, \tilde{G}_L the degrees of freedom associated with the interior coarse grid points in $\tilde{\Omega}_L$, and \tilde{G}_G the degrees of freedom associated with the remaining coarse

grid nodes as shown in Figure 1. For convenience, we define the shell grid outside the local region as $\hat{G} = \tilde{G}_I \cup \tilde{G}_G$ so that $\tilde{G} = \hat{G} \cup \tilde{G}_L$. Finally, the composite grid, denoted as G^C is defined as follows:

$$G^C = \hat{G} \cup G_L \quad (3)$$

For information transfer between the two levels, we employ the prolongation operator \tilde{Q} , which is partitioned into two blocks for convenience. The first block, denoted by \hat{Q} , relates the degrees-of-freedom in \hat{G} to those corresponding to the interface degrees of freedom of G , i.e. G_I :

$$\hat{Q} : \hat{G} \rightarrow G_I \quad (4)$$

where

$$\hat{Q} = \begin{bmatrix} \tilde{Q}_I & 0 \end{bmatrix} \quad (5)$$

such that

$$\tilde{Q}_I : \tilde{G}_I \rightarrow G_I \quad (6)$$

Likewise, we define the second block of the prolongation operator, denoted by \bar{Q} , which correlates the information between $\tilde{G}_I \cup \tilde{G}_L$ and the internal degrees of freedom of G , i.e. G_L :

$$\bar{Q} : \tilde{G}_I \cup \tilde{G}_L \rightarrow G_L \quad (7)$$

which is partitioned as

$$\bar{Q} = \begin{bmatrix} \tilde{Q}_{LI} & \tilde{Q}_{LL} \end{bmatrix} \quad (8)$$

such that

$$\tilde{Q}_{LI} : \tilde{G}_I \rightarrow G_L \text{ and } \tilde{Q}_{LL} : \tilde{G}_L \rightarrow G_L \quad (9)$$

Consequently, the operator \tilde{Q} can be structured as follows:

$$\tilde{Q} = \begin{bmatrix} \tilde{Q}_I & 0 & 0 \\ \tilde{Q}_{LI} & \tilde{Q}_{LL} & 0 \end{bmatrix} \quad (10)$$

The restriction operators $\tilde{Q}^*:G \rightarrow \tilde{G}$ and $\hat{Q}^*:G_I \rightarrow \hat{G}$ are transposed of \tilde{Q} and \hat{Q} , respectively.

For subsequent derivations we will introduce the following notation:

$$\tilde{u} = [\tilde{u}_I \tilde{u}_L \tilde{u}_G]^* \text{ where } \tilde{u}_I \in \tilde{G}_I, \tilde{u}_L \in \tilde{G}_L, \tilde{u}_G \in \tilde{G}_G.$$

$$\hat{u} = [\hat{u}_I \hat{u}_G]^* \text{ where } \hat{u} \in \hat{G}.$$

$$u = [\hat{Q}\hat{u} u_L]^* \text{ where } u_L \in G_L.$$

$$\tilde{A} = \begin{bmatrix} \tilde{A}_{II} & \tilde{A}_{IL} & \tilde{A}_{IG} \\ \tilde{A}_{LI} & \tilde{A}_{LL} & 0 \\ \tilde{A}_{GI} & 0 & \tilde{A}_{GG} \end{bmatrix} \text{ stiffness matrix on } \tilde{G}.$$

$$\hat{A} = \begin{bmatrix} \tilde{A}_{II} & \tilde{A}_{IG} \\ \tilde{A}_{GI} & \tilde{A}_{GG} \end{bmatrix} \text{ stiffness matrix on } \hat{G}.$$

$$A = \begin{bmatrix} A_{II} & A_{IL} \\ A_{LI} & A_{LL} \end{bmatrix} \text{ stiffness matrix on } G.$$

$\tilde{f} = [\tilde{f}_I \tilde{f}_L \tilde{f}_G]$ force vector, where $\tilde{f}_I, \tilde{f}_L, \tilde{f}_G$ are nodal forces acting on grids $\tilde{G}_I, \tilde{G}_L, \tilde{G}_G$, respectively.

$\hat{f} = [\hat{f}_I \hat{f}_G]^*$ force vector acting on \hat{G} .

$f = [f_I f_L]$ where f_I and f_L are nodal forces acting on grids G_I and G_L , respectively.

We note that the displacement vectors \tilde{u} and \hat{u} are related via orthogonal operator L given by

$$T = \begin{bmatrix} I & 0 & 0 \\ 0 & 0 & I \end{bmatrix} \quad (11)$$

where I is an identity matrix of an appropriate size, such that

$$\hat{u} = T\tilde{u} \quad (12)$$

We now may formulate an algebraic system of equations for the two-level linear problem. It consists of finding a pair of nodal displacements vectors (\hat{u}, u) such that

$$1/2((\hat{A}\hat{u}, \hat{u}) + (Au, u)) - (\hat{f}, \hat{u}) - (f, u) \Rightarrow \min_{(\hat{u}, u)} \quad (13)$$

where (\cdot, \cdot) denotes the bilinear form defined by

$$(u, v) = \sum_{j=1}^n u_j v_j \quad u, v \in R^n \quad (14)$$

Minimization of (13) with respect to (\hat{u}, u) subjected to the interface condition (13) yields a system of linear equations on the composite grid:

$$\begin{bmatrix} (\hat{A} + \hat{Q}^* A_{II} \hat{Q}) & \hat{Q}^* A_{IL} \\ A_{LI} \hat{Q} & A_{LL} \end{bmatrix} \begin{bmatrix} \hat{u} \\ u_L \end{bmatrix} = \begin{bmatrix} \hat{f} + \hat{Q}^* f_I \\ f_L \end{bmatrix} \quad (15)$$

The system of linear equations (15) can be solved either directly or iteratively. It is our objective to develop a hierarchical global-local procedure, which exploits the solution of the auxiliary shell model on the entire problem domain.

2.2 Two-level solution procedures

In this section, we describe a four-step procedure for solving the system of linear equations (15). The iterative solution procedure based on minimization of energy functional (13) is given below:

Step 1

Find the correction $\delta\tilde{u}^i$ which minimizes the two-level energy functional (13) on the subspace of the coarse grid functions:

$$\begin{aligned} & \frac{1}{2}((\hat{A}(\hat{u}^i + T\delta\tilde{u}^i), \hat{u}^i + T\delta\tilde{u}^i) + (A(u^i + \tilde{Q}\delta\tilde{u}^i), u^i + \tilde{Q}\delta\tilde{u}^i)) - \\ & (\hat{f}, \hat{u}^i + T\delta\tilde{u}^i) - (f, u^i + \tilde{Q}\delta\tilde{u}^i) \Rightarrow \min_{\delta\tilde{u}^i} \end{aligned} \quad (16)$$

where the superscripts refer to the iteration count. Note that the coarse grid correction $\delta\tilde{u}$ has a similar partitioning to \tilde{u} , i.e.,

$$\delta \tilde{u} = \left[\delta \tilde{u}_I \quad \delta \tilde{u}_L \quad \delta \tilde{u}_G \right]^* \quad \text{and} \quad \delta \hat{u} = \left[\delta \tilde{u}_I \quad \delta \tilde{u}_G \right]^* .$$

The direct minimization of (16) with respect to $\delta \tilde{u}$ yields:

$$(T^* \hat{A} T + \tilde{Q}^* A \tilde{Q}) \delta \tilde{u}^i = T^* (\hat{f} - \hat{A} \hat{u}^i) + \tilde{Q}^* (f - A u^i) \quad (17)$$

The first term $T^* \hat{A} T$ on the left-hand side represents the assembled form of the coarse grid stiffness matrix, whereas the second term $\tilde{Q}^* A \tilde{Q}$ represents the restricted stiffness matrix of the 3D elasticity model in the local region. For the purpose of approximating the coarse grid correction $\delta \tilde{u}$ we will replace the two terms by the stiffness matrix of the shell model on the entire problem domain, i.e.,

$$\tilde{A} \Leftarrow T^* \hat{A} T + \tilde{Q}^* A \tilde{Q} \quad (18)$$

Substitution (18) represents a major departure from the classical FAC method. In fact, this approximation may not be necessarily good because there might be a significant difference between the two mathematical models for thin domain elasticity problems (see for example [12]). Nevertheless, this approximation is absolutely must if the composite grid method is to be considered as a viable alternative to engineering global-local approaches in aerospace industries. A typical all-shell grid \tilde{G} often consists of over a million degrees-of-freedom, whereas local grids G constructed in the vicinity of cutouts, fasteners, holes and other interconnects are orders of magnitude smaller. In a large scale computational environment this approximation will significantly reduce computational cost, since only a single factorization of \tilde{A} is required for numerous redesigns of local features.

Step 2

Once the coarse grid correction has been carried out, it is necessary to update the solution:

$$\tilde{u}^{i+1} = \tilde{u}^i + \delta \tilde{u}^i \quad \hat{u}^{i+1} = \hat{u}^{i+1} + T \delta \tilde{u}^i \quad u^{i+1} = u^i + \tilde{Q} \delta \tilde{u}^i. \quad (19)$$

Step 3

Find the correction Δu_L on the fine mesh, which minimizes the energy functional on the subspace of the functions on G_L , i.e. keeping \hat{u}^i fixed

$$\frac{1}{2} ((\hat{A} \hat{u}^i, \hat{u}^i) + (A(u^i + \Delta u^i), u^i + \Delta u^i)) - (\hat{f}, \hat{u}^i) - (f, u^i + \Delta u^i) \Rightarrow \min_{\Delta u^i} \quad (20)$$

where $\Delta u_I = 0$ to maintain compatibility.

The direct minimization of (20) yields

$$A_{LL}\Delta u_L^i = f_L - A_{LI}\hat{Q}\hat{u}^i - A_{LL}u_L^i \quad (21)$$

If (21) is solved exactly, i.e.

$$\Delta u_L^i = A_{LL}^{-1}(f_L - A_{LI}\hat{Q}\hat{u}^i - A_{LL}u_L^i) \quad (22)$$

then the corresponding iterative process will be referred as HFAC-ex. Alternatively, A_{LL} can be replaced by preconditioner P_{LL} , which yields

$$\Delta u_L^i = \tau_i P_{LL}^{-1}(f_L - A_{LI}\hat{Q}\hat{u}^i - A_{LL}u_L^i) \quad (23)$$

where τ_i is a relaxation parameter given by

$$\tau_i = \frac{(f_L - A_{LI}\hat{Q}\hat{u}^i - A_{LL}u_L^i, v_L^i)}{(A_{LL}v_L^i, v_L^i)} \quad (24)$$

and $v_L^i = P_{LL}^{-1}(f_L - A_{LI}\hat{Q}\hat{u}^i - A_{LL}u_L^i)$. The latter will be referred as HFAC-ap.

Step 4

Since the approximation introduced in (18) is not necessarily good, we view steps 1-3 as a nonsymmetric preconditioner, and thus displacements \tilde{u}^i , \hat{u}^i , u^i computed in step 2 are updated using a two-parameter acceleration scheme. For convenience, the total correction on the fine grid, i.e. $\tilde{Q}\delta\tilde{u}^i + \Delta u^i$, is denoted here by du^i . Then, we ultimately update the solution according to

$$\begin{aligned} \tilde{u}^{i+1} &= \tilde{u}^i + \alpha\delta\tilde{u}^i + \beta\delta\tilde{u}^{i-1} \\ \hat{u}^{i+1} &= \hat{u}^i + \alpha T\delta\tilde{u}^i + \beta T\delta\tilde{u}^{i-1} \\ u^{i+1} &= u^i + \alpha du^i + \beta du^{i-1} \end{aligned} \quad (25)$$

where the parameters α , β are found from the minimization of the energy functional on the subspace spanned by the vectors $[(T\delta\tilde{u}^i)_G du^i]^*$ and $[(T\delta\tilde{u}^{i-1})_G du^{i-1}]^*$:

$$\begin{aligned} &\frac{1}{2}((\hat{A}(\hat{u}^i + \alpha T\delta\tilde{u}^i + \beta T\delta\tilde{u}^{i-1}), \hat{u}^i + \alpha T\delta\tilde{u}^i + \beta T\delta\tilde{u}^{i-1}) + \\ &(A(u^i + \alpha du^i + \beta du^{i-1}), u^i + \alpha du^i + \beta du^{i-1})) - \\ &(\hat{f}, \hat{u}^i + \alpha T\delta\tilde{u}^i + \beta T\delta\tilde{u}^{i-1}) - (f, u^i + \alpha du^i + \beta du^{i-1}) \Rightarrow \min_{\alpha, \beta} \end{aligned} \quad (26)$$

A direct minimization of (26) with respect to α and β yields:

$$\begin{bmatrix} c_{11} & c_{12} \\ c_{12} & c_{22} \end{bmatrix} \begin{bmatrix} \alpha \\ \beta \end{bmatrix} = \begin{bmatrix} r_1 \\ r_2 \end{bmatrix} \quad (27)$$

where

$$\begin{aligned} c_{11} &= (T^* \hat{A} T \delta \tilde{u}^i, \delta \tilde{u}^i) + (Adu^i, du^i) \\ c_{22} &= (T^* \hat{A} T \delta \tilde{u}^{i-1}, \delta \tilde{u}^{i-1}) + (Adu^{i-1}, du^{i-1}) \\ c_{12} &= (T^* \hat{A} T \delta \tilde{u}^i, \delta \tilde{u}^{i-1}) + (Adu^i, du^{i-1}) \\ r_1 &= (T^* (\hat{f} - \hat{A} \hat{u}^i), \delta \tilde{u}^i) + (f - Au^i, du^i) \\ r_2 &= (T^* (\hat{f} - \hat{A} \hat{u}^i), \delta \tilde{u}^{i-1}) + (f - Au^i, du^{i-1}) \end{aligned} \quad (28)$$

2.3 Intergrid transfer operators

Let P_A be the finite element node in the 3D solid mesh at the interface Ω_I and let P_{A_i} represent its degrees-of-freedom with $P_{A_\alpha} = \begin{bmatrix} P_{A_1} & P_{A_2} \end{bmatrix}$ corresponding to in-plane degrees-of-freedom and P_{A_3} to the transverse normal degrees-of-freedom. Likewise, \tilde{P}_a denotes the nodes in the shell model at the interface $\tilde{\Omega}_I$ having either 5 or 6 degrees-of-freedom per node.

We will construct the interface prolongation operator $\tilde{Q}_I : \tilde{G}_I \rightarrow G_I$ (needed for both HFAC-ex and HFAC-ap procedures) assuming the so-called ‘‘telescopic’’ constraints at the shell/3D interface, where the inplane degrees-of-freedom $P_{A_\alpha} \in \Omega_I$ and transverse degrees-of-freedom at the midplane $\{P_{A_3}(\zeta = 0)\} \in \Omega_I$ are considered as the slave nodes, i.e., belong to the set G_I , whereas the transverse degrees-of-freedom outside the midplane $\{P_{A_3}(\zeta) \neq 0\} \in \Omega_I$ belong to the set G_L rather than G_I . Here, for simplicity, we assume that there exists a layer of nodes in the 3D solid mesh at the midplane, as shown in Figure 1.

The interface prolongation operator \tilde{Q}_I consists of nodal blocks Q_I^{Aa} corresponding to mapping the solution from the coarse mesh node \tilde{P}_a to P_A , where the projection of the fine grid node P_A onto the shell surface is within the shell element connected to node \tilde{P}_a . Using the shell element formulation based on the degenerated solid model, the nodal interface prolongation operator Q_I^{Aa} in the local fiber coordinate system is given by

$$Q_I^{Aa} = \begin{bmatrix} \tilde{N}_a(\xi_A, \eta_A) & 0 & 0 & 0 & \frac{1}{2}h_A\zeta_A\tilde{N}_a(\xi_A, \eta_A) \\ 0 & \tilde{N}_a(\xi_A, \eta_A) & 0 & -\frac{1}{2}h_A\zeta_A\tilde{N}_a(\xi_A, \eta_A) & 0 \\ 0 & 0 & \tilde{N}_a(\xi_A, \eta_A) & 0 & 0 \end{bmatrix} \quad (29)$$

Note that the first three columns correspond to translational degrees-of-freedom, whereas columns 4 and 5 correspond to rotational degrees of freedom in the fiber coordinate system. The first two rows correspond to the prolongation of the in-plane degrees of freedom, whereas row three designates prolongation at the midplane in the transverse direction. $\tilde{N}_a(\xi_A, \eta_A)$ denotes the in-plane shape function corresponding to the shell element node \tilde{P}_a computed at the fine grid node P_A ; ξ_A, η_A, ζ_A are the natural coordinates in the shell computed at fine grid node P_A .

If the HFAC-ap scheme is employed, then, in addition to \tilde{Q}_I it is necessary to construct the prolongation operator $\bar{Q}: \tilde{G}_I \cup \tilde{G}_L \rightarrow G_L$. Let \hat{Q}^{Aa} be the initial value of nodal blocks \bar{Q}^{Aa} in the fiber coordinate system obtained from the degenerated solid model in a similar fashion to that in equation (29). Since the lower order shell theories [12] do not take into account the fiber elongation in the transverse normal direction, it is necessary to correct the transverse normal displacements by the integral over transverse normal strains. The resulting nodal prolongation operator in the fiber coordinate system is given as

$$\bar{Q}^{Aa} = \hat{Q}^{Aa} - \begin{bmatrix} 0 \\ 0 \\ \sum_{i=1}^5 \int_{\bar{\theta}}^{\zeta_A} \frac{D_{6i}\tilde{\mathbf{B}}_{ai}(\xi_A, \eta_A)}{D_{66}} d\zeta \end{bmatrix} \quad (30)$$

where \mathbf{D} is the three-dimensional constitutive matrix corresponding to the transverse normal stress, and $\tilde{\mathbf{B}}_{ai}$ is the block of the strain-displacement matrix of the shell element corresponding to the shell node \tilde{P}_a .

3.0 Model problem

In this section the rate of convergence of the iterative procedure described in the previous section is estimated in the closed form for beam-2D model problem shown in Figure 2.

For the 2D domain on $-L \leq x_1 \leq L$, $-H \leq x_2 \leq H$ the governing elasticity equations in the tensorial notation are given as:

$$\sigma_{ij,j} + b_i = 0 \quad \sigma_{ij} = \lambda u_{k,k} \delta_{ij} + 2\mu u_{(i,j)} \quad i, j = 1, 2 \quad (31)$$

where λ, μ are material constants; σ_{ij} the symmetric stress tensor; δ_{ij} the Kronecker delta; comma denotes the spatial derivative; parentheses around the subscripts represent the symmetric gradient.

For the beam domain on $L < x_1 \leq 2L$, $-2L \leq x_1 < -L$ the governing elasticity equations are the same, but in addition, the following Timoshenko beam constraints are imposed to restrict the kinematics of the beam:

$$\sigma_{i2} = 0 \quad u_1(x_1, x_2) = -\theta(x_1)x_2 \quad \int_{-H}^H x_2 dx_2 = 0 \quad (32)$$

where θ is the beam rotation. The essential boundary conditions are applied at the two ends of the beam, i.e., $u_1(x_1 = \mp 2L) = -\theta(x_1 = \mp 2L) = 0$. Compatibility is enforced at the beam-2D interface:

$$\begin{aligned} u_1(x_1 = \mp L) &= -\theta(x_1 = \mp L)x_2 \\ u_2(x_1 = \mp(L + \varepsilon)) &= u_2(x_1 = \mp(L - \varepsilon), x_2 = 0) \quad 0 < \varepsilon \ll 1 \end{aligned} \quad (33)$$

3.1 Model description

We consider the finite element discretization depicted in Figure 2. On the global level we use Timoshenko's beam elements with quadratic shape functions for the transverse displacements and linear shape functions for the rotations. Timoshenko's beam element has been chosen since it represents one-dimensional counterpart of the Mindlin/Reissner shell/plate element. For the local model, a single p -type 2-D element is employed with nonuniform polynomial order of displacement interpolation functions in x and y denoted as p and q , respectively.

We first focus on the construction of the discrete system of equations for the model problem. The displacement field of the 2D element can be cast into the following form:

$$u_i = \sum_{J=1}^4 U_{iJ} a_J \quad (34)$$

where $\mathbf{a} = [v_1 \ \theta_1 \ v_2 \ \theta_2]^*$ is the vector of nodal displacements (two translations and two rotations), and U_{iJ} , $i = 1, 2$, $J = 1, 4$, is the solution of the two-dimensional problem corresponding to the prescribed J -th unit nodal displacement while keeping the other nodal displacements constrained. Note that the constraints between the beam and the 2-D element are of telescopic type, i.e., at the interface u_1 is prescribed for all y , while u_2 is prescribed only at $y = 0$. It is not the objective of this paper to study the influence of various global/local interface conditions on the solution accuracy. Instead, we are only focusing on the convergence characteristics of the iterative process given the interface conditions employed in practical applications [27].

The functions U_{iJ} are discretized as follows:

$$U_{iJ} = \sum_l \sum_m d_{iJlm} \Phi_l(\xi) \Psi_m(\eta) \quad (35)$$

where $\xi = \frac{1}{L}$ and $\eta = \frac{1}{H}$, $\Phi_l(\xi)$ and $\Psi_m(\eta)$ are the basis functions given as

$$\begin{aligned} \Phi_1 &= -\frac{\xi-1}{2} & \Phi_2 &= \frac{\xi+1}{2} \\ \Phi_{k+1} &= \sqrt{\frac{2k-1}{2}} \int_{-1}^{\xi} P_{k-1}(t) dt & k &= 2, 3, \dots \end{aligned} \quad (36)$$

and

$$\Psi_n = \eta^{n-1} \quad n = 1, 2, \dots \quad (37)$$

where $P_k(\xi)$ are Legendre polynomials of order k .

Let $\mathbf{K} \mathbf{d}_{iJ} = 0$ be the discrete system of equations arising from the discretization given in (35) subjected to J -th unit displacement on the boundary, where $\mathbf{d}_{iJ} = \{d_{iJlm}\}$ and \mathbf{K} is the corresponding stiffness matrix. The coefficients d_{iJlm} may be found exactly or approximately. The former is denoted as HFAC-ex, while the latter is termed HFAC-ap.

Once the coefficients d_{iJlm} are found, one may find the coefficients of the stiffness matrix for 2-D element with the interface nodal degrees of freedom $\mathbf{a} = [v_1 \ \theta_1 \ v_2 \ \theta_2]^*$:

$$A_{JK} = \int_{\Omega_e} U_{(aJ,b)} D_{abfg} U_{(fK,g)} d\Omega_e \quad (\text{sum over repeated indices}) \quad (38)$$

where $J = 1 \dots 4$, $K = 1 \dots 4$, D_{abfg} are the components of the 2D plain-strain elastic constitutive tensor, $u_{(i,j)}$ are the components of the symmetric part of the tensor $\nabla \mathbf{u}$.

3.2 Convergence properties of the algorithm

The point iteration matrix $S: e_I^i \rightarrow e_I^{i+1}$ derived in the Appendix is given as

$$S = I - \tilde{Q} \tilde{A}^{-1} \tilde{Q}^* A \quad (39)$$

where e_I^i is the solution error at the interface in iteration i and \tilde{Q} is the prolongation operator \tilde{Q} equal to

$$\tilde{Q} = \begin{bmatrix} 1 & 0 & 0 & 0 & 0 & 0 \\ 0 & 1 & 0 & 0 & 0 & 0 \\ 0 & 0 & 1 & 0 & 0 & 0 \\ 0 & 0 & 0 & 1 & 0 & 0 \end{bmatrix} \quad (40)$$

More details on equations (39) and (40) are given in the Appendix.

In this section, we present closed form expressions for the spectral radius of the iteration matrices for different values of p and q , denoted by $\rho(S^{p,q})$, where p is the in-plane polynomial order (x_1 direction) and q is the polynomial order through the thickness of the beam (x_2 direction). These expressions have been obtained using the symbolic math package Maple [28]. In what follows we give a Taylor series expansions about the point $H/L = 0$, where $\nu < 0.5$ is Poisson's ratio.

3.2.1 HFAC-ex algorithm

$$\rho(S^{2,1}) = \frac{2}{33}(1-\nu)\left(\frac{H}{L}\right)^{-2} + \frac{2}{5445} \frac{1375\nu^2 + 1504\nu - 752}{1-2\nu} + O\left(\left(\frac{H}{L}\right)^2\right) \quad \text{for } \nu \leq 0.497$$

$$\rho(S^{2,1}) = \frac{2}{3} \left(\frac{v^2}{1-2v} \right) \text{ otherwise.}$$

$$\rho(S^{3,1}) = \frac{8(1+v)(1-3v)}{33(1-2v)} + O\left(\left(\frac{H}{L}\right)^2\right) \text{ for } v \leq 0.277$$

$$\rho(S^{3,1}) = \frac{2}{3} \left(\frac{v^2}{1-2v} \right) \text{ otherwise.}$$

$$\rho(S^{2,2}) = \frac{2}{33}(1-v)\left(\frac{H}{L}\right)^{-2} - \left(\frac{1343}{4840} + \frac{19}{396}v\right) + O\left(\left(\frac{H}{L}\right)^2\right)$$

$$\rho(S^{2,3}) = \frac{2}{33}(1-v)\left(\frac{H}{L}\right)^{-2} - \left(\frac{1343}{4840} + \frac{19}{396}v\right) + O\left(\left(\frac{H}{L}\right)^2\right)$$

$$\rho(S^{3,2}) = \frac{8}{33} - \frac{4}{1815} \frac{(33v^2 - 330v + 406)}{1-v} \left(\frac{H}{L}\right)^2 + O\left(\left(\frac{H}{L}\right)^4\right)$$

It can be seen that the HFAC-ex method for the model problem converges ($\rho(S) < 1$) independently of material parameters, provided $p \geq 3$ and $q \geq 2$. In the case of linear through-the-thickness discretization, the iterative process diverges independently of in-plane discretization as the material approaches the incompressible limit, i.e., $v \rightarrow 0.5$.

Similarly, in the case of insufficient in-plane discretization ($p < 3$), HFAC-ex diverges for thin shells ($\frac{H}{L} \rightarrow 0$).

3.2.2 HFAC-ap algorithm

We first consider a Gauss Seidel preconditioner of the form $(l + d)^{-1}$, where l is the lower triangular part of A_{LL} in (21), and d is the main diagonal of A_{LL} .

$$\rho(S^{2,1}) = \frac{2}{33}(1-v)\left(\frac{H}{L}\right)^{-2} + \frac{2}{5445} \frac{1375v^2 + 1504v - 752}{1-2v} + O\left(\left(\frac{H}{L}\right)^2\right) \text{ for } v \leq 0.497$$

$$\rho(S^{2,1}) = \frac{2}{3} \left(\frac{v^2}{1-2v} \right) \text{ otherwise.}$$

$$\rho(S^{3,1}) = \frac{7}{100}(1-v)\left(\frac{H}{L}\right)^{-2} + \frac{99v^2 - 98v + 49}{1-2v} + O\left(\left(\frac{H}{L}\right)^2\right)$$

$$\rho(S^{2,2}) = \frac{2}{33}(1-\nu)\left(\frac{H}{L}\right)^{-2} + \frac{1}{557568}\left(\frac{87362\nu^2 + 286437\nu - 154609}{1-2\nu}\right) + \mathcal{O}\left(\left(\frac{H}{L}\right)^2\right)$$

$$\rho(S^{2,3}) = \frac{2}{33}(1-\nu)\left(\frac{H}{L}\right)^{-2} + \frac{1}{557568}\frac{87362\nu^2 + 286437\nu - 154609}{1-2\nu} + \mathcal{O}\left(\left(\frac{H}{L}\right)^2\right)$$

$$\rho(S^{3,2}) = \frac{7}{100}(1-\nu)\left(\frac{H}{L}\right)^{-2} + \frac{1}{600}\frac{177\nu^2 - 784\nu + 392}{1-2\nu} + \mathcal{O}\left(\left(\frac{H}{L}\right)^2\right) .$$

For large values of Poisson's ratio $\nu \rightarrow 0.5$, higher order terms in H/L cannot be truncated since they contain terms of the form $\frac{1}{(1-2\nu)^n}$ ($n > 0$) that grow unboundedly for incompressible materials, thereby affecting the spectral radius considerably even for small values of H/L .

For all cases considered the spectral radius was $\mathcal{O}\left(\left(\frac{H}{L}\right)^{-2}\right)$, indicating that HFAC-ap scheme with fixed number of smoothing iterations is inappropriate for thin shells. Next, we investigate whether stronger smoothing, in the form of two symmetric Gauss-Seidel sweeps, which correspond to the preconditioner $(l+d)^{-1}d(l+d)^{-T}$, can eliminate the lower order term.

$$\rho(S^{2,1}) = \frac{2}{33}(1-\nu)\left(\frac{H}{L}\right)^{-2} + \frac{2}{5445}\frac{1375\nu^2 + 1504\nu - 752}{1-2\nu} + \mathcal{O}\left(\left(\frac{H}{L}\right)^2\right) \quad \text{for } \nu \geq 0.497$$

$$\rho(S^{2,1}) = \frac{2}{3}\left(\frac{\nu^2}{1-2\nu}\right) \quad \text{otherwise.}$$

$$\rho(S^{3,1}) = \frac{1}{99}(1-\nu)\left(\frac{H}{L}\right)^{-2} + \frac{1}{16335}\frac{11000\nu^2 + 8654\nu - 4327}{1-2\nu} + \mathcal{O}\left(\left(\frac{H}{L}\right)^2\right)$$

For the case of $p = 3, q = 1$ we also consider the SSOR preconditioner of the form

$$\omega(2-\omega)(l+d)^{-1}d(l+d)^{-T} \quad , \text{ which yields}$$

$$\rho(S_{\omega}^{3,1}) = \frac{1-\nu}{99}(5\omega^6 - 30\omega^5 + 90\omega^4 - 160\omega^3 + 180\omega^2 - 120\omega + 36)\left(\frac{H}{L}\right)^{-2} + \mathcal{O}(1)$$

with $\omega = 1$ giving the optimal choice.

$$\rho(S^{2,2}) = \frac{2(1-\nu)}{33} \left(\frac{H}{L}\right)^{-2} + \frac{1}{1393920} \frac{284240\nu^2 + 681608\nu - 385739}{1-2\nu} + O\left(\left(\frac{H}{L}\right)^2\right)$$

$$\rho(S^{2,3}) = \frac{2(1-\nu)}{33} \left(\frac{H}{L}\right)^{-2} + O(1)$$

$$\rho(S^{3,2}) = \frac{1}{99}(1-\nu) \left(\frac{H}{L}\right)^{-2} + O(1) \quad .$$

For all the polynomial orders p, q considered, the SSOR preconditioner reduced considerably the coefficient of the term $O\left(\left(\frac{H}{L}\right)^{-2}\right)$ as compared to GS preconditioner even though, this term was not completely removed.

In our last experiment conducted on the model problem, we have perturbed the stiffness matrix of the local grid (2D element) with a small fraction ($\eta \rightarrow 0$) of its diagonal, i.e:

$$A^{new} = A + \eta \text{diag}(A) \quad (41)$$

and then have solved the local problem exactly. The resulting spectral radius has been symbolically computed using MAPLE:

$$\rho(S_{\eta}^{3,1}) = \left[\frac{10}{9}(1-\nu)\eta^2 + O(\eta^3) \right] \left(\frac{H}{L}\right)^{-2} + O(1) \quad (42)$$

It can be seen that a small perturbation of the exact local factor has a devastating influence as $H/L \rightarrow 0$, since a typical L/H ratio is over 1000 in aerospace and mechanical engineering applications and over 100 in civil engineering applications. This phenomenon is a direct consequence of the approximation introduced in (18).

4.0 Numerical Examples

Two problems are considered for numerical investigation of computational efficiency of HFAC-ex and HFAC-ap procedures in the context of shell/3D global-local problems. The first test problem is a thick laminated shell subjected to axial tension. The second is a thin cylindrical shell. In both cases, local effects developed at the free edge are of interest.

As a termination criterion, we use the ratio of the residual norm versus the norm of the right-hand side vector, i.e.,

$$\|r\|_2 / \|f\|_2 \leq eps \quad \text{and} \quad \|v\|_2 = \left(\sum_{i=1}^n v_i^2 \right)^{0.5} \quad (43)$$

where the tolerance is chosen to be $eps = 10^{-6}$. All computations have been carried out on a SUN SPARC 10/41 workstation.

4.1 (45/-45)_s laminate in extension

We consider a thick four-layer (45/-45)_s laminate subjected to axial tension. Geometry, boundary conditions and material properties are shown in Fig. 3. The plies in the laminate are of equal thickness idealized as a homogeneous, orthotropic material. Subscript ‘1’ denotes the direction parallel to the fibers, subscript ‘2’ for in-plane direction perpendicular to the fibers, and subscript ‘3’ for the out-of-plane direction.

ANS shell elements [29] are used in the global region and 10-node tetrahedrals in the local region. The local mesh is graded towards the free edge of the laminate. On the coarse mesh, the number of nodes is 171 and the number of shell finite elements is 36. On the fine mesh, the number of nodes is 11530 and the number of tetrahedral elements is 7233. For HFAC-ap we employ an Incomplete Cholesky Factorization preconditioner by value with zero fill-ins. Table 1 compares convergence of the HFAC-ap and HFAC-ex algorithms. It can be seen that although the number of cycles required for HFAC-ap is significantly higher than for HFAC-ex, the CPU time for HFAC-ap is lower. This example suggest that for thick domain problems, where $(L/H)^2$ term is not dominant, HFAC-ap with a relatively weak coarse grid preconditioner is an optimal choice.

4.2 Isotropic cylindrical shell problem

In this subsection, we study a thin isotropic cylindrical shell problem. Geometry, displacement boundary conditions, material properties are depicted in Fig. 4.

As in the previous example, ANS shell elements are placed in the global region, whereas a 10-node tetrahedral unstructured mesh is used in the local region. The coarse model consists of 171 nodes and 36 shell elements. For the fine model three meshes were considered: (i) 226 10-node tetrahedral finite elements (467 nodes), (ii) 980 10-node tetrahedral finite elements (1820 nodes), 3318 10-node tetrahedral finite elements (5840 nodes). All fine level meshes have the same number of 3D elements through the thickness direction (approximately 2 elements), whereas the number of elements is approximately varied by a factor of 2 in the in-plane direction for the 3D meshes considered. The coarsest mesh of 3D elements has the size of a 3D element in the inplane direction roughly the same as that of the shell element. Tables 2-4 provide the information on convergence characteristics for the three fine meshes considered. It can be seen that, by increasing the number of the elements in the inplane directions, both HFAC-ex and HFAC-ap converge faster. This phenomenon is in good agreement with our analytical convergence estimates in Section 3. Moreover, numerical experiments reveal that the convergence of HFAC-ap with a weak course grid preconditioner is very poor. This finding confirms our analytical studies in Section 3 indicating that for thin beams or shells the $(L/H)^2$ term completely dominates the convergence characteristics of the HFAC-ap scheme, unless the coarse grid problem is solved up to a very tight tolerance.

5.0 Conclusions

A hierarchical version of the composite grid method (denoted as HFAC-ex and HFAC-ap), which exploits the solution of the shell model in studying local effects via 3D solid model, is developed. Convergence studies on a beam/2D model problem indicate that the spectral radius of the point iteration matrix for HFAC-ex method is $O(1)$, whereas for HFAC-ap it is $O((L/H)^2)$, where L and H are the span and the thickness of the beam, respectively. Numerical experiments in multidimensions confirm these findings.

The major departure between the present paper and the work pioneered by McCormick [14],[30] is in the approximation introduced in equation (18). This approximation may not be necessarily good because there might be a significant difference between the shell and the 3D models for thin domain elasticity problems. A typical all-shell grid \tilde{G} often consists of over a million degrees-of-freedom, whereas local grids G constructed in the local regions requiring better resolution are orders of magnitude smaller. Thus the approximation (18) will significantly reduce the computational cost, since only a single factorization of A is required for numerous redesigns of local features.

As a by-product of the approximation introduced in (18), two factors have been found to be absolutely critical to maintain reasonable rates of convergence of the iterative process for thin domain problems:

- i. *The local problem has to be solved exactly or up to a very tight tolerance.* For our numerical model, the thin cylindrical shell problem, it took 377-1615 cycles for the MIC smoother by value, with up to 20 fill ins and 5 smoothings to converge as opposed to 11-25 cycles with a direct solver. In our analytical model we have found that a small perturbation to the exact local factor has a devastating influence on the convergence as $H/L \rightarrow 0$.
- ii. *The two parameter acceleration in the two step scheme.* It is necessary to consider a single cycle of the HFAC method as a nonsymmetric preconditioner and to accelerate the iterative process with a two parameter acceleration scheme rather than with a more popular conjugate gradient method. None of the numerical examples considered converges without acceleration. In fact they rapidly diverge, as opposed to better than 0.5 rate of convergence with the two parameter acceleration scheme. This is because the 3D model is typically much stiffer than a shell model resulting in a poor preconditioning.

6.0 References

- 1 J. Fish, S. Markolefas, R. Guttal, and P. Nayak, "On adaptive multilevel superposition of finite element meshes for linear elastostatics." *Appl. Numer. Math.*, 14, 135-164 (1994).
- 2 J. Fish, "The s-version of the finite element method", SCOREC report \#18-1990, Rensselaer Polytechnic Institute Troy, NY-12180; and *Comput. and Struct.*, 43, 539-547(1990)
- 3 J. Fish, "Hierarchical modeling of discontinuous fields." *Comm. Appl. Numer. Methods*, 8, 443-453 (1992).

- 4 J. Fish and S. Markolefas, "The s-version of the finite element method for multilayer laminates" *Int. J. Numer. Methods Eng.*, 33, 1081-1105(1992).
- 5 J. Fish and R. Guttal, "The p-version of Finite Element Method for Shell Analysis." *Comp. Mech. Int. Journal*, 16, 1-13 (1995).
- 6 J.Fish and R.Guttal, "The s-version of Finite Element Method for Laminated Composite Shells," accepted in *Int. J. Numer. Methods Eng.* (1995).
- 7 J. Fish and S. Markolefas, "Adaptive global-local refinement strategy based on interior error estimates of the h-method." *Int. J. Numer. Methods Eng.*, 37, 828-838, (1994).
- 8 I. Babuska, S. Stroubulis, C. S. Upadhyay and S. K. Gangaraj, "A posteriori estimation and adaptive control of the polluting error in the h-version of the finite element method." Technical note BN-1175, Institute for Physical Science and Technology, Univ. of Maryland, College Park, MD.
- 9 H. Hinnant, "A fast method of numerical quadrature for p-version finite element matrices", *A.I.A.A.*, 1386 (1993).
- 10 B. A. Szabo and I. Babuska, "Finite Element Analysis." Wiley. (1991).
- 11 K. C. Park, G. M. Stanley, "A curved C^0 Shell element based on Assumed Natural Coordinate Strains." *J. of Appl. Mech.*, 108, 278-290(1986).
- 12 T. J. R. Hughes, "The Finite Element Method." Prentice-Hall. (1987).
- 13 R. E. Bank, T. F. Dupont and H. Yserentant, "The hierarchical basis multigrid method." *Numer. Math.*, 52, 427-458 (1988).
- 14 S. F. McCormick and J. W. Thomas, "The fast adaptive composite grid (FAC) method for elliptic equations." *Mathematics of Comput.*, 46, 439-456, (1986).
- 15 J. Bramble, R. E. Ewing, J. E. Pasciak and A. H. Schatz, "A preconditioning technique for the efficient solution of problems with local grid refinement." *Comp. Meth. Appl. Mech. Eng.*, 67, 149-159 (1988).
- 16 J. E. Flaherty, P. K. Moore and C. Ozturan, "Adaptive overlapping methods for parabolic systems." in *Adaptive Methods for Partial Differential Equations* (Eds. J. E. Flaherty, P. J. Paslow, M. S. Shephard and J. D. Vasilakis), SIAM (1989).
- 17 J. D. Whitcomb, "Iterative global-local finite element analysis." *Computers and Structures*, 40, 1027-1031 (1991).
- 18 J. Fish and V. Belsky, "Multigrid method for periodic heterogeneous media. Part 2: Multiscale modeling and quality control in multidimensional case." *Comp. Meth. Appl. Mech. Eng.*, Vol. 126, pp. 17-38, ,(1995).
- 19 A. Brandt, "Multi-level adaptive solutions to boundary-value problems." *Mathematics of Computation*, 31, 333-390 (1977).

- 20 T. Belytschko, J. Fish and A. Bayliss, ``The spectral overlay on finite elements for problems with high gradients.'' *Comp. Meth. Appl. Mech. Eng.*, 81, 71-89 (1990).
- 21 H. Yserentant, ``On multilevel splitting of finite element spaces.'' *Numer. Math.*, 379-412, (1986).
- 22 J. N. Reddy and D. H. Robbins, ``Theories and computational models for composite laminates.'' *Appl. Mech. Rev.*, 47, 147-169 (1994).
- 23 A. K. Noor, W. S. Burton and J. M. Peters, ``Predictor-Corrector procedures for stress and free vibration analyses of multilayered composite plates and shells.'' *Comp. Meth. Appl. Mech. Eng.*, 82, 341-363, (1990).
- 24 N. F. Knight, J. B. Ransom, O. H. Griffin and D. M. Thompson, ``Global/Local methods research using a common structural analysis framework.'' *Finite Element Analysis and Design*, 9, 91-112 (1991).
- 25 K. M. Mao and C. T. Sun, ``A refined global-local finite element analysis method.'' *Int. J. Numer. Methods Eng.*, 32, 29-43 (1991).
- 26 J. Fish, V. Belsky and M. Pandheeradi, ``Composite grid method for hybrid systems.'' accepted in *Comp. Meth. Appl. Mech. Eng.*, (1995).
- 27 ABAQUS Theory Manual, Version 5.4, Hibbitt, Karlsson & Sorensen, Inc., 1994.
- 28 MAPLE V, Release 3, Waterloo Maple Software, 1994.
- 29 K.C.Parks and G,Stanley, 'A curved C^0 shell element based on assumed natural coordinate strains,' *Journal of Applied Mechanics*, Vol. 108, 1986, pp.278-290.
- 30 S. McCormick, "Multilevel Adaptive Methods for Partial Differential Equations," SIAM Frontiers, III, 1987.

7.0 Appendix: Derivation of the point iteration matrix

In this section, we derive the point iteration matrix $S: e_I^i \rightarrow e_I^{i+1}$ for the model problem given in Section 3.1, where the subscript i denotes the iteration count. For the model problem described in 3.1, we condensed out the internal degrees of freedom of the local grid yielding $e_I = \hat{e}_I$. Also \tilde{G}_G can be excluded from the consideration due to the boundary conditions prescribed at the end points of the beam. Under these circumstances, the prolongation operator \tilde{Q} in (10) can be simplified if we define it as the operator relating the nodal displacements in $\tilde{G}_I \cup \tilde{G}_L$ to those in G_I , i.e. $\tilde{Q}: \tilde{G}_I \cup \tilde{G}_L \rightarrow G_I$, where \tilde{Q} is given in equation (40).

The errors in the two subsequent iterations are related as follows

$$e_I^{i+1} = e_I^i - \tilde{Q}\delta\tilde{u}^i \quad (44)$$

Combining (39) with (16) with exact Jacobians replaced by \tilde{A} yields

$$e_I^{i+1} = e_I^i - \tilde{Q}\tilde{A}^{-1}(T^*(\hat{f}_I - \hat{A}_{II}\hat{u}_I^i) + \tilde{Q}^*(f_I - Au_I^i)) \quad (45)$$

where T is defined as $T = \begin{bmatrix} I & 0 \end{bmatrix}$ and I is identity matrix of an appropriate size. Since $T = \tilde{Q}$ and $\hat{u}_I = u_I$, equation (44) may be written as

$$e_I^{i+1} = e_I^i - \tilde{Q}\tilde{A}^{-1}\tilde{Q}^*(\hat{A}_{II} + A)e_I^i \quad (46)$$

Defining

$$A = \hat{A}_{II} + A \quad (47)$$

where A , once again, is determined according to (38), one can write

$$e_I^{i+1} = Se_I^i \quad (48)$$

where the iteration matrix S is equal to

$$S = I - \tilde{Q}\tilde{A}^{-1}\tilde{Q}^*A \quad (49)$$

FIGURE 1. Partitioning of the shell-3D global-local model

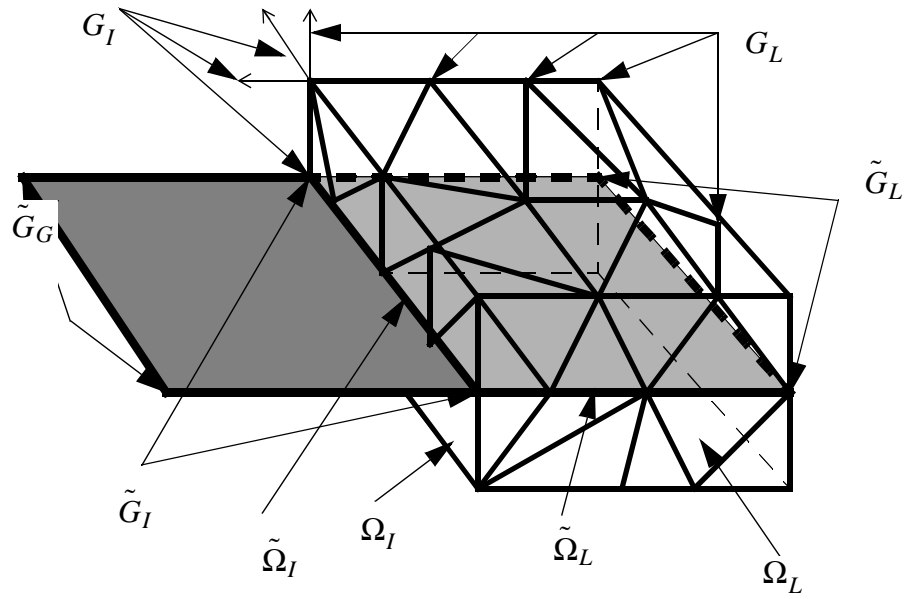


FIGURE 2. Discretization of the model problem

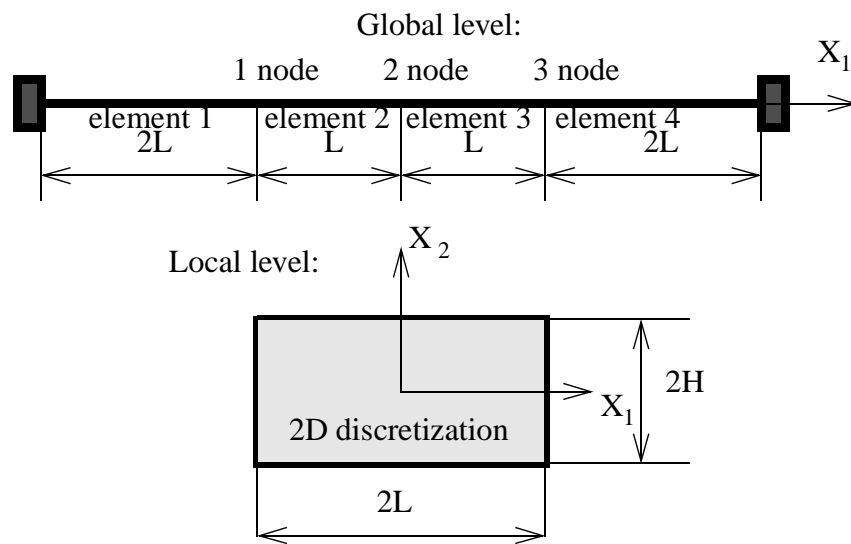
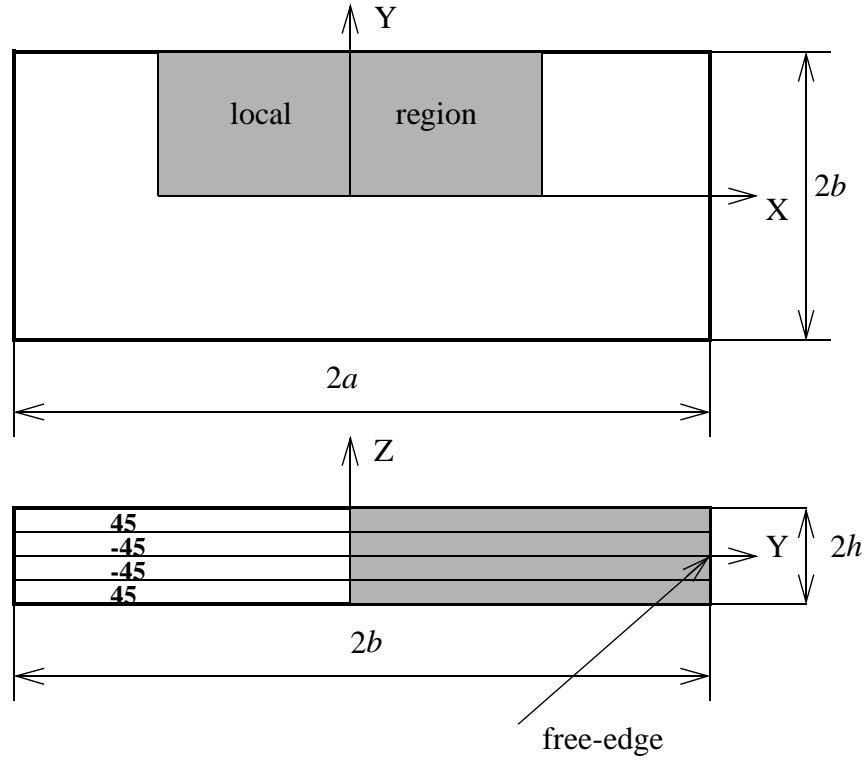


FIGURE 3. Axial tension problem definition



$$\frac{a}{b} = 10, \frac{b}{h} = 4, h = 2h_k, \frac{b}{h_k} = 8$$

$$E_1 = 20 \times 10^6 \text{ psi}, E_2 = E_3 = 2.1 \times 10^6 \text{ psi}$$

$$G_{12} = G_{23} = G_{13} = 0.85 \times 10^6 \text{ psi}$$

$$\nu_{12} = \nu_{23} = \nu_{13} = 0.21$$

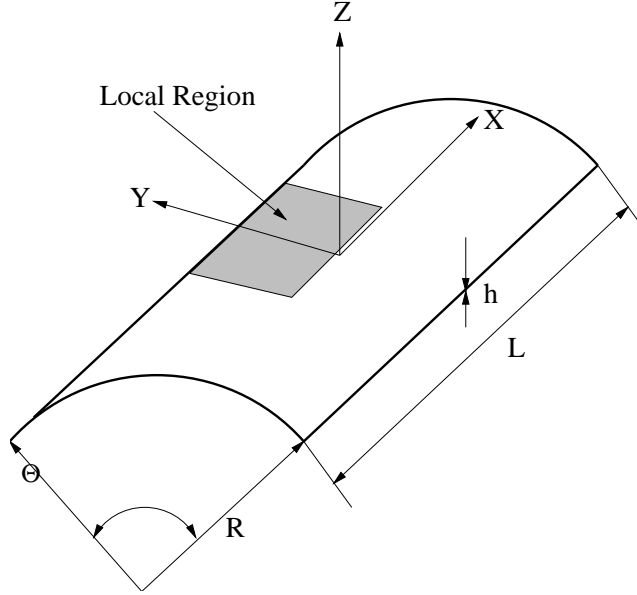
displacement boundary conditions:

$$u_1(a, y, z) = u_0 \quad u_1(-a, y, z) = 0$$

$$u_2(-a, 0, z) = u_2(a, 0, z) = 0$$

$$u_3(-a, 0, z) = 0$$

FIGURE 4. Cylindrical shell problem definition



$$L = 675\text{mm}, R = 300\text{mm}, h = 3\text{mm}, \Theta = \frac{\pi}{2}$$

$$E = 26\text{GPa}, \nu = 0.3$$

displacement boundary conditions:

$$u_1\left(-\frac{L}{2}, y, z\right) = 0 \quad u_1\left(\frac{L}{2}, y, z\right) = 1\text{mm}$$

$$u_2\left(-\frac{L}{2}, 0, z\right) = u_2\left(\frac{L}{2}, 0, z\right) = 0$$

$$u_3\left(-\frac{L}{2}, 0, z\right) = 0$$

TABLE 1. Convergence studies for laminated plate problem

Method Type	Number of relaxation sweeps (HFAC-ap)	Number of Cycles	CPU(sec) factorization	CPU(sec) iterative solution	CPU(sec) total
HFAC-ap	1	57	30	274	800
HFAC-ap	2	38	30	250	776
HFAC-ap	3	31	30	247	774
HFAC-ap	4	28	30	265	800
HFAC-ap	5	24	30	264	788
HFAC-ex	-	10	595	85	1050

TABLE 2. Convergence studies for cylindrical shell problem (226 elements in the fine grid)

Method Type	Number of relaxation sweeps (HFAC-ap)	Number of Cycles	CPU(sec) factorization	CPU(sec) iterative solution	CPU(sec) total
HFAC-ap	5	1615	0.8	726	760
HFAC-ex	-	25	1.3	5	33

TABLE 3. Convergence studies for cylindrical shell problem (980 elements in the fine grid)

Method Type	Number of relaxation sweeps (HFAC-ap)	Number of Cycles	CPU(sec) factorization	CPU(sec) iterative solution	CPU(sec) total
HFAC-ap	5	580	3	1143	1240
HFAC-ex	-	14	16	12	100

TABLE 4. Convergence studies for cylindrical shell problem (3318 elements in the fine grid)

Method Type	Number of relaxation sweeps (HFAC-ap)	Number of Cycles	CPU(sec) factorization	CPU(sec) iterative solution	CPU(sec) total
HFAC-ap	5	377	14	2690	2980
HFAC-ex	-	11	179	24	364